Ceramics International 48 (2022) 12654–12659

Contents lists available at ScienceDirect

Ceramics International

journal homepage: www.elsevier.com/locate/ceramint

Green synthesis of a $YBa_2Cu_3O_7$ ceramic superconductor using the fruit extract of *Juniperus phoenicea*

Imad Hamadneh [a,*], Ahmed Al-Mobydeen [b], Yousef Al-Dalahmeh [c], Rula Albuqain [d], Shorouq Alsotari [d], Omar H. Al-Obaidi [e], Borhan Albiss [f], Ammar H. Al-Dujaili [g]

[a] Chemistry Department, Faculty of Science, University of Jordan, 11942, Amman, Jordan
[b] Department of Chemistry, Faculty of Science, Jerash University, Jerash, 26150, Jordan
[c] Chemistry Department, Faculty of Science, Isra University, PO Box 33 Isra University Office 11622, Amman, Jordan
[d] Cell Therapy Center (CTC), University of Jordan, 11942, Amman, Jordan
[e] Department of Chemistry, College of Science, University of Anbar, Ramadi, Iraq
[f] Bio-Medical Physics Laboratory, Jordan University of Science and Technology, Irbid, 22110, Jordan
[g] Hamdi Mango Center for Scientific Research, University of Jordan, 11942, Amman, Jordan

ARTICLE INFO

Keywords:
Electrical properties
Juniperus phoenicea
Green chemistry
Perovskites
Superconductivity
Grain boundaries

ABSTRACT

Plant extracts have gained significant attention as an eco-friendly method to synthesize metal and metal oxide NPs. The products usually consist of single-component metals and are rarely used for polyatomic ceramics. This study highlights the synthesis of a $YBa_2Cu_3O_7$ superconductor using Arar fruit extract (*Juniperus phoenicea*). The formation of metal complexes was recorded and monitored via FTIR as an indication of capping and stabilizing of the metal complexes. The product was calcined at 900 °C for 10 h, pelletized, sintered at 920 °C for 15 h under oxygen flow and then cooled to room temperature with a cooling rate of 2 °C/min. XRD confirmed the phase formation of the superconducting phase where the Y123% exceeded 91%. The electrical transport behavior for the prepared Y123 showed metallic behavior with an offset temperature, $T_{C(R\ =\ 0)}$ (89 K), in a single step. Using plant extracts for green synthesis is an eco-friendly method that simplifies ceramic synthesis and can be scaled up for bulk and industrial applications.

1. Introduction

$REBa_2Cu_3O_{7-\delta}$ or RE123 ceramic superconductors (RE = Y, La, Er, Nd, Pr, Dy, Ho, Gd, Sm, Yb) have been extensively investigated over three decades due to their unique electrical and magnetic properties and used in different applications, such as nuclear magnetic resonance, HTSC power cables, HTSC current fault limiters, and Maglev trains [1–6]. The most popular methods used to prepare RE123 have been conventional solid-state [7] and chemical methods in recent decades. However, using a chemical process such as coprecipitation, sol-gel, and microemulsion techniques is considered a method to save time and energy during the formation of nano-precursors, which simplifies the construction of ceramic materials since the component mixing is at the subatomic level [8–11].

Green synthesis (biogenic method) has gained significant attention for synthesizing metallic and metal oxide NPs employing several organisms, such as fungi, yeast, bacteria, plant extracts, and macro- and micronutrients (proteins, peptides, vitamins) [12]. It acts as a capping and reducing agent due to the different functional groups obtained from natural surfactants, reduced sugars, proteins, and polyphenols [13]. In addition, water acts as a solvent and a reaction medium; thus, it is considered an eco-friendly or green method. It is employed to prepare Au, Ag, Pt, CuO, ZnO, ZnO, Fe_2O_3, and NiO [14–19]. Arar (*Juniperus phoenicea*) is a Mediterranean plant that grows in Jordan and other countries, such as Sinai of Egypt, Algeria, Libya, Spain, Cyprus, and Saudi Arabia. These trees are 6–10 m in height and live in the mountains. For centuries, the fruits and leaves have been used in traditional medicine, and recently, laboratory experiments have shown excellent biological activities against bacteria and cancer cells. The fruit extract of Arar can be a potential template for nanomaterials and ceramic synthesis due to the different functional groups obtained from natural surfactants, reduced sugars, proteins, and polyphenols [20,21]. For example, amentoflavone, gallic acid, and rutin found in *Juniperus phoenicea* are rich in hydroxyl groups which are responsible for

* Corresponding author.
E-mail address: i.hamadneh@ju.edu.jo (I. Hamadneh).

https://doi.org/10.1016/j.ceramint.2022.01.135
Received 2 October 2021; Received in revised form 1 January 2022; Accepted 13 January 2022
Available online 21 January 2022

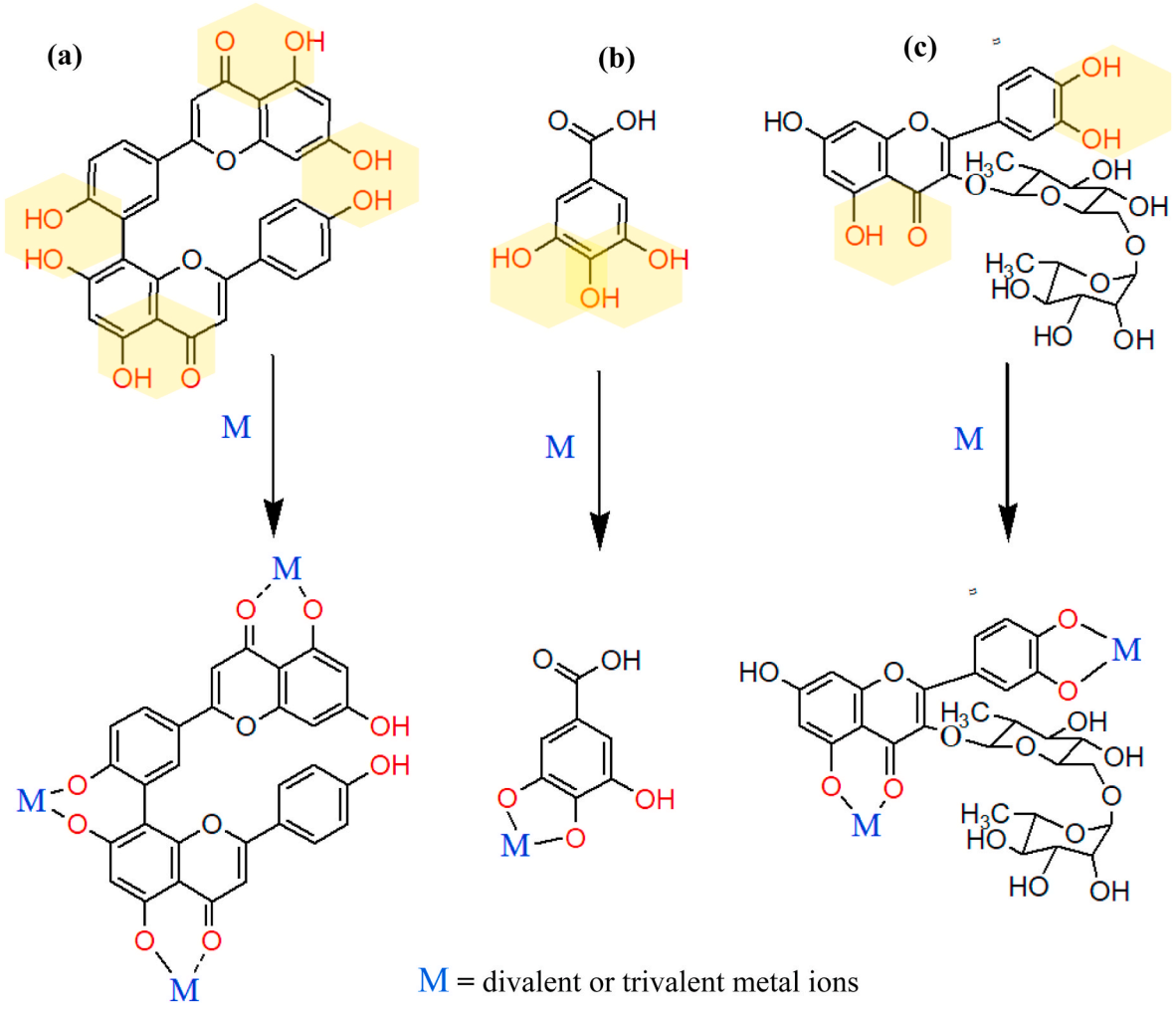

Fig. 1. Metal-chelating active sites (highlighted in yellow) in (a) amentoflavone, (b) gallic acid, and (c) rutin. (For interpretation of the references to colour in this figure legend, the reader is referred to the Web version of this article.)

metal-binding activity (Fig. 1).

In previous studies, yttrium oxide (Y_2O_3), barium carbonate ($BaCO_3$), copper oxide (CuO), zinc oxide (ZnO), titanium oxide (TiO_2), silver (Ag), and gold (Au) nanoparticles have been synthesized using *Azadirachta indica* (Neem) extract [22–24].

In this work, Y123 was prepared by the green method using an aqueous extract of *Juniperus phoenicea*. The resulting materials were characterized using FTIR, TGA, XRD, SEM, and electrical testing techniques.

2. Experimental

2.1. Preparation of Juniperus phoenicea extract

The preparation of the plant extract was carried out by boiling (50) g of dried fruit powders in (500) cm^3 of distilled water under vigorous mixing for (30) minutes. The sample was filtered and centrifuged for 15 min at 6000 rpm and then stored in a refrigerator for further experiments.

2.2. Preparation of $YBa_2Cu_3O_7$

The metal complex with a nominal composition of $YBa_2Cu_3O_{7-\delta}$ was synthesized by mixing yttrium(III) acetate tetrahydrate [$Y(OOCCH_3)_3.4H_2O$], barium acetate [$Ba(OOCCH_3)_2$], and copper(II) acetate monohydrate [$Cu(OOCCH_3)_2.\ H_2O$] (high purity powders ≥/99.9% supplied by Sigma Aldrich) with water to form an aqueous solution. A 10.0 mL aliquot of plant extract solution was added gradually to the mixed metal acetate solution under vigorous steering for 3 h at 80 °C until the formation of a dried brown precipitate. The brown powders were kept overnight at 80 °C and then calcined at 900 °C in air for 12 h to remove the remaining volatile materials. The calcined powders were reground in a marble mortar for 10 min, pressed into pellets with a diameter of ~12.5-mm and a thickness of 2 mm under a load of 6 tons using a hydraulic press model Carver and then sintered at 920 °C under oxygen flow for 15 h and slowly cooled to room temperature at 2 °C/min.

2.3. Characterization

The metal complexes and their oxide powders were characterized using a Fourier transform infrared (FTIR) technique using a PerkinElmer model Spectrum Two FTIR spectrophotometer equipped with an attenuated total reflection (ATR) sampling accessory. The samples were examined by X-ray powder diffraction with a Cu $K_{\alpha 1}$ radiation source (λ = 1.54056 Å) using a Shimadzu 7000 X-ray diffraction system at 40 kV and 30 mA with a step of 0.02° over the range 4–60°. The electrical resistance property was measured using the standard four-point probe technique in the range 80.0–150.0 K using 1.0 mA (DC) using cryostat system model Janis VNF. Morphological studies were obtained using field-emission scanning electron microscopy with an FEI-Versa 3D STEM attachment model. The electrical resistance property was measured

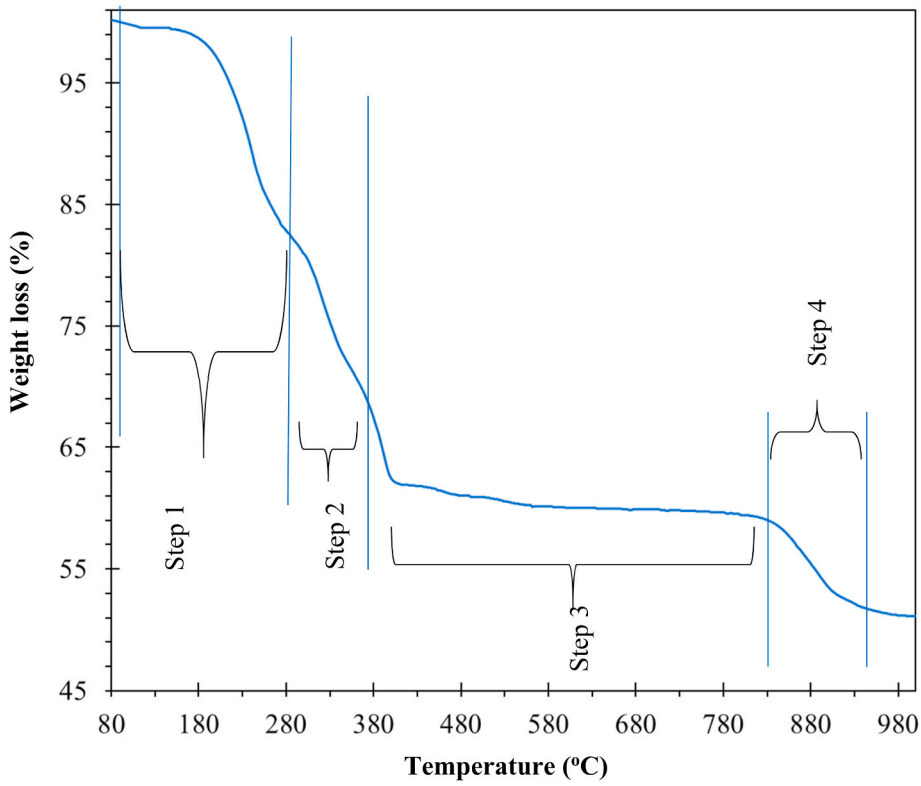

Fig. 2. Thermogravimetric analysis (TGA) of a green mixture of Y, Ba, and Cu. (For interpretation of the references to colour in this figure legend, the reader is referred to the Web version of this article.)

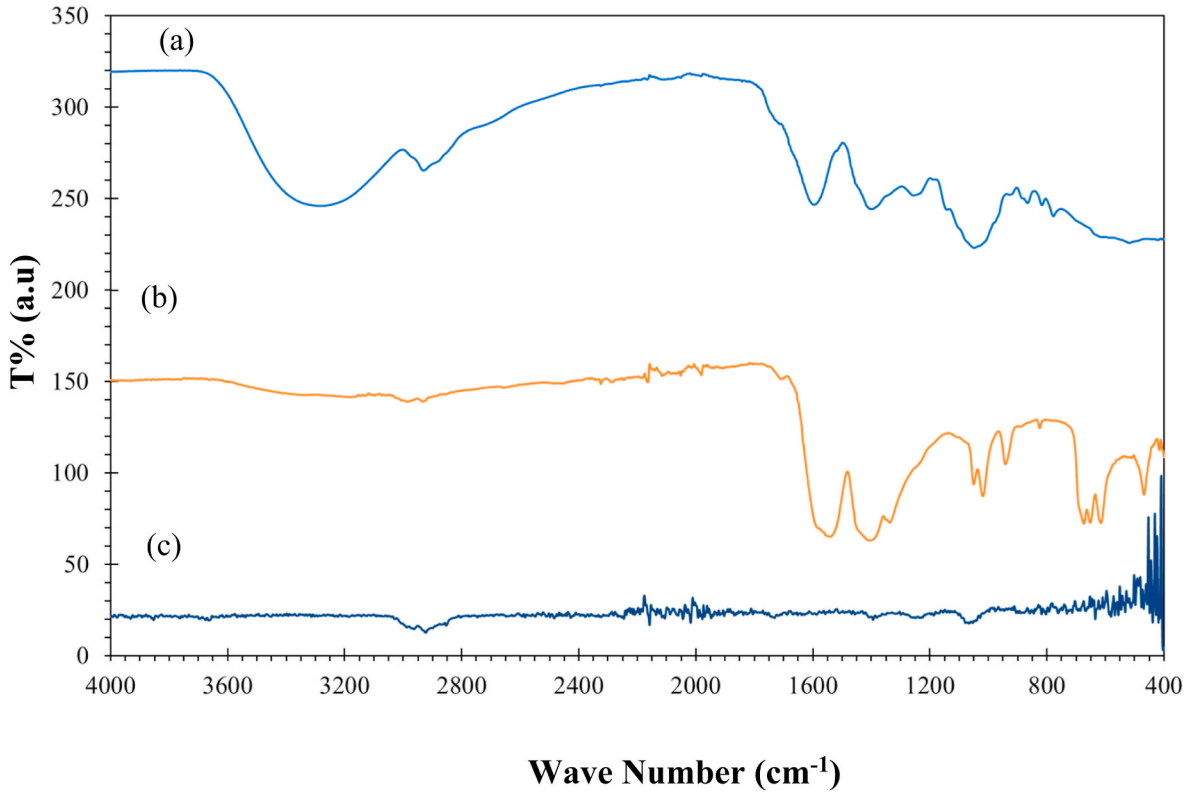

Fig. 3. FTIR spectra of the (a) *Juniperus phoenicea* extract; (b) green mixture of Y, Ba, and Cu; and (c) YBCO ceramic. (For interpretation of the references to colour in this figure legend, the reader is referred to the Web version of this article.)

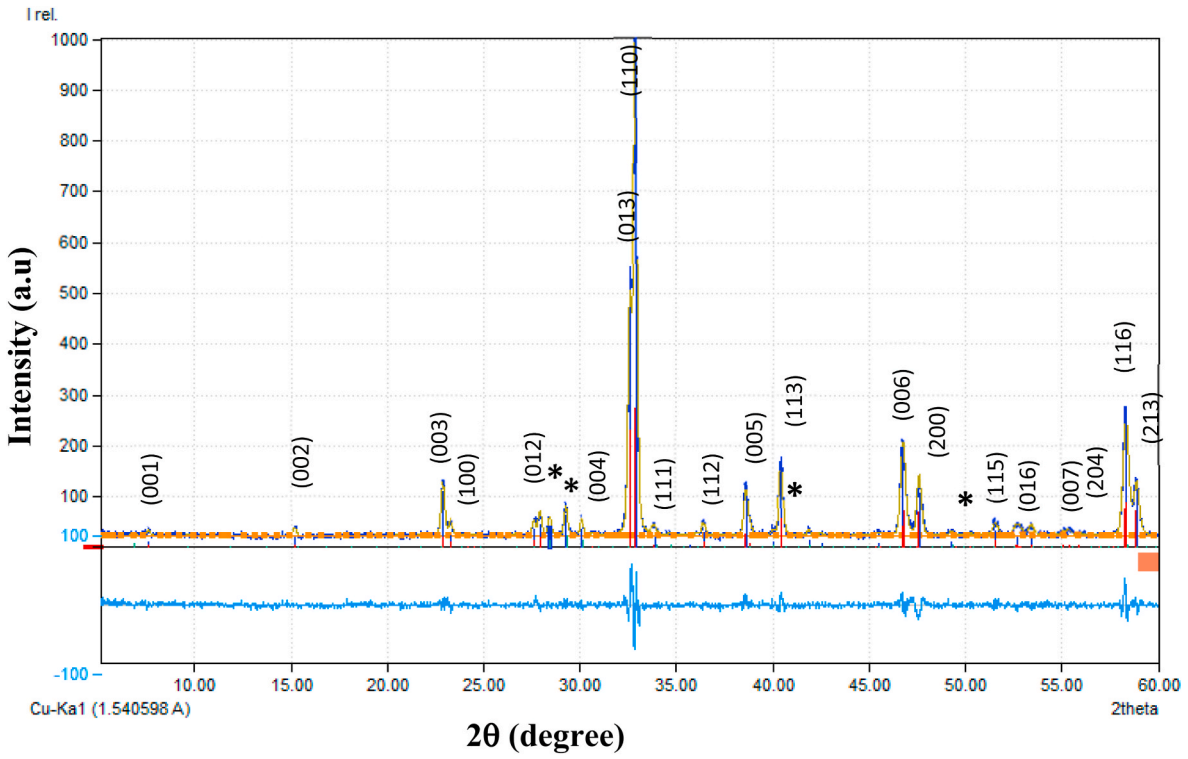

Fig. 4. XRD pattern of Y123 using *Juniperus phoenicea* as a green template. (*h k l*): Y123, *: 211 and 011 phases. Normalized resistance as a function of. (For interpretation of the references to colour in this figure legend, the reader is referred to the Web version of this article.)

using the standard four-point probe technique at varying temperatures (80.0–150.0 K) using cryostat system model Janis VNF. Morphological studies were recorded using a FEI-Versa 3D field-emission scanning electron microscope.

3. Results and discussion

Thermogravimetric analysis (TGA) of a green precursor (Fig. 2) showed four weight-loss steps (drops) as a function of temperature. The first weight drop, the moisture, and the water within the crystals end at approximately 280 °C. The second drop in weight shows the decomposition of the Cu complex, Ba complex, and Y complex to form CuO, $BaCO_3$, and Y_2O_3, respectively. The deterioration of $BaCO_3$ to BaO is presented at the third drop. The final weight loss shows complete decomposition and the formation of $YBa_2Cu_3O_{7-\delta}$ that begins at approximately 900 °C. TGA results suggest an excellent calcination and sintering temperature in the range of 900–920 °C.

FTIR spectra for the Arar extract, green mix of Y–Ba–Cu ions with plant extract and sintered $YBa_2Cu_3O_{7-\delta}$ ceramics were recorded and are presented in Fig. 3. FTIR reveals the functional groups that might act as stabilizers or capping agents. It has been noted that the plant extract displayed the same functional groups represented in the green mix. The bands in the range 469–823 cm^{-1} in the green mix correspond to the metal-oxygen of organometallic formation bonds, the bands at 779, 814, 868 and 922–1261 cm^{-1} in the plant extract correspond to the stretching vibration of the C–C of alkanes and the C–O–C of ethers, and the peaks in the range 1261–1395 cm^{-1}, 1396-1416 cm^{-1} are due to the C–H aldehyde, and C═C stretching modes, respectively. The bands that appeared at 1546-1599 cm^{-1} and 1740-1745 cm^{-1} represented the C═O carboxylic anion and ketone stretching modes. Finally, the peaks at 2923 cm^{-1} and 3338 cm^{-1} belong to the (O–H) of the phenol and water groups in stretching mode [22–27]. However, no significant peaks were observed for the YBCO ceramic since all the abovementioned functional groups were decomposed during the heating process at 920 °C.

Fig. 4 shows the XRD patterns for the sintered Y123. All the identified peaks at 7.58°, 15.18°, 22.86°, 22.9°, 23.28°, 24.16°, 27.60°, 30.64°, 32.59°, 32.89°, 33.80°, 36.41°, 38.57°, 40.43°, 45.57°, 46.70°, 47.60°, 51.57°, 52.63°, 54.07°, 55.09°, 57.68°, 58.30°, and 58.87° were assigned to the (0 0 1), (0 0 2), (0 0 3), (0 1 0), (1 0 0), (0 1 1), (0 1 2), (0 0 4), (0 1 3), (1 1 0), (1 1 1), (1 1 2), (0 0 5), (1 1 3), (1 1 4), (0 0 6), (2 0 0), (1 1 5), (0 1 6), (2 1 1), (0 0 7), (2 0 4), (1 1 6), and (2 1 3) planes that belong to the orthorhombic structure of the Y123 phase (JCPDS, #01-078-2143), which was analyzed via the Rietveld method using Match 3! software; the results are summarized in Table 1, including the following: the Pmmm space group, No. 47, Z = 1, α = β = γ = 90°. The measured lattice parameters are $a = 3.8175 \pm 0.0001$ Å, $b = 3.8790 \pm 0.0002$ Å, and $c = 11.6594 \pm 0.0008$ Å. The density of the lattice is $d = 6.409$ g/cm^3 with an estimated ±0.009 precision. Few peaks belonging to impurities 28.42°, 29.27°, 30.08°, 35.68°, 39.99°, 41.87°, 42.54° and 49.27° were also detected and belonged to the nonsuperconducting phases $BaCuO_2$ (Y011) and Y_2BaCuO_5 (Y211). The Y123% was found to be 91.3% and calculated using Equation (1) [28]:

$$Y_{123}\% = \Sigma I_{123} / (\Sigma I_{123} + \Sigma I_{Impurities}) \quad (1)$$

Table 1
Summarized data based on Rietveld analysis for $YBa_2Cu_3O_7$: lattice parameters, crystallite size, crystal structure, goodness of fit (GOF), and agreement factors (Bragg-R- Factor, RF-Factor and χ^2).

Parameter	value
a (Å)	3.8175 ± 0.0001
b (Å)	3.8790 ± 0.0002
c (Å)	11.6594 ± 0.0008
Volume (Å^3)	172.651 ± 0.016
123%	91.30(.99)
GoF-index	1.1
Bragg R-factor	2.84
RF-factor	2.7
χ^2	1.32

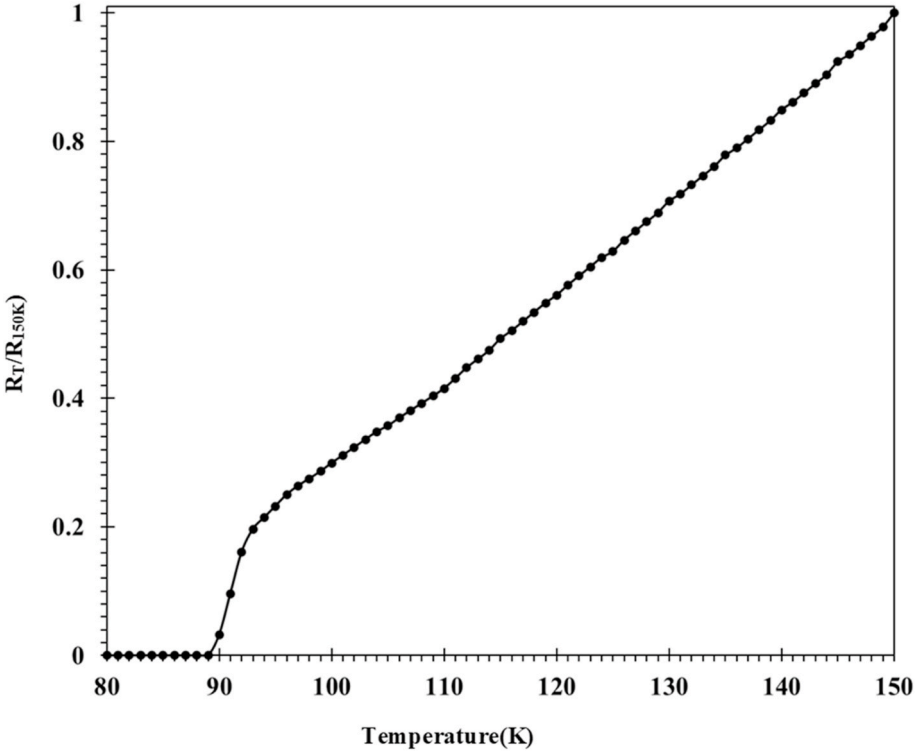

Fig. 5. Normalized resistance of Y123 as a function of temperature.

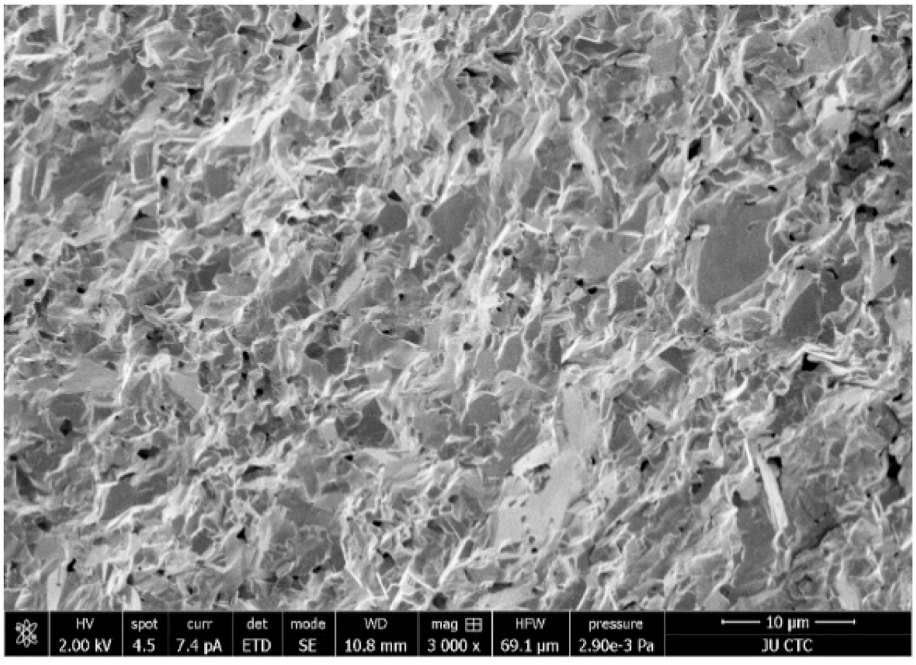

Fig. 6. SEM micrographs of the Y123 fracture surface.

Where *I* is the peak intensity of the observed phases.

The measured DC electrical resistance as a function of temperature (R-T) for sintered Y123 (Fig. 5) presented normal metallic behavior with a single-step transition feature. The zero-resistance temperature $T_{C(R=0)}$ and onset temperature ($T_{C\text{-onset}}$) were 89.0 K and 93.0 K, respectively. The ΔT_C, which is $T_{C\text{-onset}}$-$T_{C(R=0)}$, was 4 K. Additionally, no sharp drop in the curve at $T_{C\text{-onset}}$ was observed due to the formation of impurities that might act as insulators and form weak links at grain boundaries. The temperature dependence of the resistivity showed a negative curvature at 110K, which might resulting from the increase in fluctuation conductivity (FLC).

SEM micrographs (Fig. 6) displayed the Y123 morphology, which was highly compacted and randomly distributed. The grain size was above 20 µm, which is considered a typical feature of Y123.

4. Conclusion

A $YBa_2Cu_3O_{7-\delta}$ superconducting ceramic was prepared with Arar

fruit extract (*Juniperus phoenicea*) and metal acetate as the starting precursors. The formation of metal complexes was recorded and monitored via FTIR spectroscopy as an indication of the capping and stabilizing of the metal complexes. XRD confirmed the phase formation of the superconducting phase where the Y123% exceeded 91%. The electrical transport behavior for the prepared Y123 showed metallic behavior with an offset temperature ($T_{C(R\ =\ 0)}$) of 89 K. Using arar extract to produce multicomponent ceramic is an environmental-friendly, and no toxic chemicals are required. In addition, it is an alternative method for ceramic production and can be scaled up to the industrial scale in nanocatalysts, superconducting magnets, and power cables.

Declaration of competing interest

The authors declare that they have no known competing financial interests or personal relationships that could have appeared to influence the work reported in this paper.

Acknowledgment

The authors would like to thank the Deanship of Scientific Research at the University of Jordan for their support.

References

[1] T. Krekels, H. Zou, G. Van Tendeloo, D. Wagener, M. Buchgeister, S.M. Hosseini, P. Herzog, Ortho II structure in $ABa_2Cu_3O_{7-\delta}$ compounds (A=Er, Nd, Pr, Sm, Yb), Phys. C Supercond. Appl. 196 (1992) 363–368, https://doi.org/10.1016/0921-4534(92)90458-O.

[2] J.D. Jorgensen, D.G. Hinks, P.G. Radaelli, S. Pei, P. Lightfoot, B. Dabrowski, C. U. Segre, B.A. Hunter, Defects, defect ordering, structural coherence and superconductivity in the 123 copper oxides, Phys. C Supercond. Appl. 185–189 (1991) 184–189, https://doi.org/10.1016/0921-4534(91)91970-F.

[3] M. Buchgeister, P. Herzog, S.M. Hosseini, K. Kopitzki, D. Wagener, Oxygen evolution from $ABa_2Cu_3O_{7-\delta}$ high-Tc superconductors with A=Yb, Er, Y, Gd, Eu, Sm, Nd and La, Phys. C Supercond. Appl. 178 (1991) 105–109, https://doi.org/10.1016/0921-4534(91)90164-T.

[4] T. Plackowski, C. Sułkowski, D. Włosewicz, J. Wnuk, Effect of the RE^{3+} ionic size on the $REBa_2Cu_3O_{7-\delta}$ ceramics oxygenated at 250 bar, Phys. C Supercond. Appl. 300 (1998) 184–190, https://doi.org/10.1016/S0921-4534(98)00133-6.

[5] R. Nagarajan, R. Vijayaraghavan, L. Ganapathi, R.A. Mohan Ram, C.N.R. Rao, Evidence for two distinct orthorhombic structures associated with different Tc regimes in $LnBa_2Cu_3O_{7-\delta}$ (Ln = Nd, Eu, Gd and Dy): a study of the dependence of superconductivity on oxygen stoichiometry, Phys. C Supercond. Appl. 158 (1989) 453–457, https://doi.org/10.1016/0921-4534(89)90243-8.

[6] B.A. Albiss, I.M. Obaidat, Applications of YBCO-coated conductors: a focus on the chemical solution deposition method, Mater. Chem. 20 (2010) 1836–1845, https://doi.org/10.1039/B917294G.

[7] I. Hamadneh, I. Abdullah, S.A. Halim, R. Abd-Shukor, Dynamic magnetic properties of superconductor/polymer NdBCO/PVC composites, J. Mater. Sci. Lett. 21 (2002) 1615–1617, https://doi.org/10.1023/A:1020377818076.

[8] M. Mujaini, S.Y. Yahya, I. Hamadneh, R. Abd Shukor, Synthesis of $YBa_2Cu_3O_{7-\delta}$ high temperature superconductor by coprecipitation method, in: A I P Conference Proceedings 1017, 2008, pp. 119–123, https://doi.org/10.1063/1.2940610.

[9] I. Hamadneh, N. Yaseen, Y. Abdallat, L. Hamadneh, O. Tarawneh, The sintering effect on the phase formation and transport current properties of $SmBa_2Cu_3O_{7-d}$ ceramic prepared from nano-coprecipitated precursors, J. Supercond. Nov. Magnetism 29 (2016) 829–834, https://doi.org/10.1007/s10948-015-3341-x.

[10] N. Yahya, M.H. Zakariah, Synthesis and characterization of $YBa_2Cu_3O_7$ (Y123) via sol-gel method for development of superconducting quantum interference device magnetometer, J. Nanosci. Nanotechnol. 12 (2012) 8147–8152, https://doi.org/10.1166/jnn.2012.4527.

[11] L. Wang, Y. Zhang, M. Muhammed, Synthesis of nanophase oxalate precursors of YBaCuO superconductor by coprecipitation in microemulsions, Mater. Chem. 5 (1995) 309–314, https://doi.org/10.1039/JM9950500309.

[12] S.F. Adil, M.E. Assal, M. Khan, A. Al-Warthan, M.R.H. Siddiqui, L.M. Liz-Marzán, Biogenic synthesis of metallic nanoparticles and prospects toward green chemistry, Dalton Trans. 44 (2015) 9709–9717, https://doi.org/10.1039/C4DT03222E.

[13] Y.T. Foo, A.Z. Abdullah, B.A. Horri, B. Salamatinia, Synthesis and characterisation of Y_2O_3 using ammonia oxalate as a precipitant in distillate pack coprecipitation process, Ceram. Int. 44 (2018) 18693–18702, https://doi.org/10.1016/j.ceramint.2018.07.098.

[14] A.W. Anwar, W. Ullah, R. Ahmad, A. Majeed, N. Iqbal, A. Khan, Simple and inexpensive synthesis of rGO-(Ag, Ni) nanocomposites via green methods, Mater. Technol. 30 (2015) 155–160, https://doi.org/10.1080/10667857.2015.1112588.

[15] M. Aminuzzaman, L.M. Kei, W.H. Liang, Green synthesis of copper oxide (CuO) nanoparticles using banana peel extract and their photocatalytic activities, AIP Conf. Proc. (2017), https://doi.org/10.1063/1.4979387.

[16] S. Afsheen, M.B. Tahir, T. Iqbal, A. Liaqat, M. Abrar, Green synthesis and characterization of novel iron particles by using different extracts, J. Alloys Compd. 732 (2018) 935–944, https://doi.org/10.1016/j.jallcom.2017.10.137.

[17] V. Lakkim, M.C. Reddy, R.R. Pallavali, K.R. Reddy, C.V. Reddy, Inamuddin, A. L. Bilgrami, D. Lomada, Green synthesis of silver nanoparticles and evaluation of their antibacterial activity against multidrug-resistant bacteria and wound healing efficacy using a murine model, Antibiotics 9 (2020) 1–22, https://doi.org/10.3390/antibiotics9120902.

[18] M.K. Zahran, A.A. Mohamed, F.M. Mohamed, M.H. El-Rafie, Optimization of biological synthesis of silver nanoparticles by some yeast fungi, Egypt. J. Chem. 56 (2013) 91–110, https://doi.org/10.21608/EJCHEM.2013.1078.

[19] M.N. Nadagouda, G. Hoag, J. Collins, R.S. Varma, Green synthesis of Au nanostructures at room temperature using biodegradable plant surfactants, Cryst. Growth Des. 9 (2009) 4979–4983, https://doi.org/10.1021/cg025608t.

[20] A. Bouyahyaoui, F. Bahri, A. Romane, M. Höferl, J. Wanner, E. Schmidt, L. Jirovetz, Antimicrobial activity and chemical analysis of the essential oil of Algerian Juniperus phoenicea, Nat Prod Commun 11 (2016) 519–522, https://doi.org/10.1177/1934578X1601100426.

[21] N. Nasri, N. Tlili, W. Elfalleh, E. Cherif, A. Ferchichi, A. Khaldi, S. Triki, Chemical compounds from Phoenician juniper berries (Juniperus phoenicea), Nat. Prod. Res. 25 (2011) 1733–1742, https://doi.org/10.1080/14786419.2010.523827.

[22] I. Hamadneh, H. Alhayek, A. Al-Mobydeen, A. Abu Jaber, R. Albuqain, S. Alsotari, Al- A.H. Dujaili, Green synthesis and characterization of yttrium oxide, copper oxide and barium carbonate nanoparticles using Azadirachta indica (the neem tree) fruit aqueous extract, Egypt. J. Chem. 62 (2019) 973–981, https://doi.org/10.21608/EJCHEM.2018.5281.1469.

[23] J. Anuradha, A. Tasneem, S.A. Abbasi, Green synthesis of gold nanoparticles with aqueous extracts of neem (Azadirachta indica), Res. J. Biotech. 5 (2010) 75–79.

[24] L. Lin, S.A. Starostin, S. Li, S.A. Khan, V. Hessel, Synthesis of yttrium oxide nanoparticles via a facile microplasma-assisted process, Chem. Eng. Sci. 178 (2018) 157–166, https://doi.org/10.1016/j.ces.2017.12.041.

[25] S. Guru, A.K. Bajpai, S.S. Amritphale, Influence of nature of surfactant and precursor salt anion on the microwave assisted synthesis of barium carbonate nanoparticles, J. Phys. Chem. C 120 (2020) 22895–22902, https://doi.org/10.1021/acs.jpcc.6b08267.

[26] H. Veisi, B. Karmakar, T. Tamoradi, S. Hemmati, M. Hekmati, M. Hamelian, Biosynthesis of CuO nanoparticles using aqueous extract of herbal tea (Stachys Lavandulifolia) flowers and evaluation of its catalytic activity, Sci. Rep. 11 (2021), https://doi.org/10.1038/s41598-021-81320-6, 1983.

[27] S. Saif, A. Tahir, T. Asim, Y. Chen, Plant mediated green synthesis of CuO nanoparticles: comparison of toxicity of engineered and plant mediated CuO nanoparticles towards Daphnia magna, Nanomaterials 6 (2016) 205, https://doi.org/10.3390/nano6110205.

[28] I. Hamadneh, A.M. Ahmad, M.H. Wahid, Z. Zainal, R. Abd-Shukor, Effect of nano-sized oxalate precursor on the formation of $GdBa_2Cu_3O_{7-\delta}$ Phase via coprecipitation method, Mod. Phys. Lett. B 23 (2009) 2063–2068, https://doi.org/10.1142/S0217984913501182.